European Journal of Phycology

ISSN: (Print) (Online) Journal homepage: www.tandfonline.com/journals/tejp20

Plocamiomonas psychrophila gen. et sp. nov. (Pelagophyceae, Heterokontophyta), an Arctic marine nanoflagellate characterized by microscopy, pigments and molecular phylogeny

Niels Daugbjerg, Cecilie Lara, Frederik F. Gai & Connie Lovejoy

To cite this article: Niels Daugbjerg, Cecilie Lara, Frederik F. Gai & Connie Lovejoy (2024) *Plocamiomonas psychrophila* gen. et sp. nov. (Pelagophyceae, Heterokontophyta), an Arctic marine nanoflagellate characterized by microscopy, pigments and molecular phylogeny, European Journal of Phycology, 59:4, 362-378, DOI: 10.1080/09670262.2024.2353940

To link to this article: https://doi.org/10.1080/09670262.2024.2353940

EUROPEAN JOURNAL OF PHYCOLOGY
2024, VOL. 59, NO. 4, 362–378
https://doi.org/10.1080/09670262.2024.2353940

Plocamiomonas psychrophila gen. et sp. nov. (Pelagophyceae, Heterokontophyta), an Arctic marine nanoflagellate characterized by microscopy, pigments and molecular phylogeny

Niels Daugbjerg [a], Cecilie Lara [a], Frederik F. Gai [a] and Connie Lovejoy [b]

[a]Department of Biology, University of Copenhagen, Universitetsparken 4, Copenhagen Ø 2100, Denmark; [b]Département de Biologie, Université Laval, Québec, QC G1V 0A6, Canada

ABSTRACT

During a field campaign in Baffin Bay (June, 1998), a sample dominated by small yellow brown biflagellates was collected from a small pocket of liquid water on the sea ice and established into a unialgal culture. Later it was given strain number CCMP2097 and deposited at the NCMA collection. Growth experiments over a range of temperatures and salinities indicated adaptation to variable Arctic conditions. This strain was studied here using light and transmission electron microscopy, HPLC for characterization of photosynthetic pigments and the relationship to related taxa was elucidated from molecular phylogeny. This integrative approach resulted in suggesting *Plocamiomonas psychrophila* gen. et sp. nov. the first systematically named Arctic species of the Pelagophyceae. *Plocamiomonas* had two unequally long flagella and the spherical cells measured 7.5 µm in diameter. Novel morphological characters included (1) a swelling on the mature flagellum, (2) a bi-layered theca, thin elongated arm-like structures emanating from the cell surface and (3) a thin filament above the flagellar transition region. This set of morphological characters represented a novel combination for the Pelagophyceae and together with evidence from the phylogenetic position of *Plocamiomonas* and eight uncultured cold-water pelagophytes supported the proposal of a new order Plocamiomonadales and a new family Plocamiomonadaceae.

HIGHLIGHTS

- First taxonomically named Arctic marine pelagophyte (from surface ice pocket).
- *Plocamiomonas psychrophila* clustered with cold-water uncultured pelagophytes.
- Flagellated cell covered by bi-layered theca and surface protrusions.

ARTICLE HISTORY Received 30 January 2024; Revised 30 April 2024; Accepted 5 May 2024

KEYWORDS Cold-water flagellate; light and electron microscopy; SSU rRNA; taxonomy; ultrastructure

Introduction

Since the description of the autotrophic uniflagellate *Pelagomonas calceolata* (Andersen *et al.*, 1993), the overall understanding of the Pelagophyceae has increased steadily. The systematics of the class was treated extensively by Han *et al.* (2018) and the species diversity markedly expanded due to work by Wetherbee *et al.* (2015, 2021, 2023) when they described six new genera and eight new species. The class currently comprises 23 genera and 32 species (including the new pelagophyte characterized here). These are split into two orders, the Sarcinochrysidales with two families (Chrysocystaceae with 4 genera and 9 species and Sarcinochrysidaceae with 11 genera and 15 species) and the Pelagomonadales which includes a single family (Pelagomonadaceae with 7 genera and 7 species). Table 1 brings an updated classification of the Pelagophyceae; note that 17 out of 23 well characterized genera (~74%) are monotypic. However, the species diversity is larger as clone library studies have revealed numerous uncultured taxa from cold waters in Svalbard (Tian *et al.*, 2009) and the Gulf of Finland (Majaneva *et al.*, 2012), as well as the Indian Ocean (Daugbjerg *et al.*, 2013). *Sulcochrysis biplastida* likely also belongs to the Pelagophyceae but it has not yet been analysed phylogenetically using ribosomal and/or chloroplast-encoded genes and therefore it takes a position as incertae sedis.

For three decades no single morphological synapomorphy suggested monophyly of the Pelagophyceae (Cavalier-Smith & Chao, 2006) and members of the class were combined due to phylogenetic analyses based on nuclear- and chloroplast-encoded gene sequences (e.g. Daugbjerg & Andersen, 1997; Yang *et al.*, 2012; Derelle *et al.*, 2016; Han *et al.*, 2018; Wetherbee *et al.*, 2019). This condition recently changed due to studies by Wetherbee *et al.* (2021, 2023). Using high-pressure freezing for preparing material for electron microscopy they were able to document the presence of a unique multi-layered theca in 14 pelagophytes (Wetherbee *et al.*, 2023). The thickness of the theca ranged from 20–25 nm in *Gazia saundersii* to

CONTACT Niels Daugbjerg n.daugbjerg@bio.ku.dk

Published online 10 Jul 2024

Table 1. Updated classification of class Pelagophyceae R.A.Andersen & G.W.Saunders with three orders and four families.

ORDER Sarcinochrysidales Gayral & Billard (with 2 families)	
FAMILY Chrysocystaceae M.Melkonian, H.S.Yoon & R.A.Andersen (with 4 genera, 9 species)	
	**Chrysocystis fragilis* C.S.Lobban, D.Honda & M.Chihara
	Chrysoreinhardia algicola (Reinhard) C.Billard
	C. feldmannii (Bourrelly & Magne) C.Billard & J.Fresnel
	**C. giraudii* (Derbès & Solier) C.Billard
	**C. muelleri* M.Melkonian & R.A.Andersen
	**Pituiglomerulus carpicornicus* Wetherbee
	**Sungminbooa australiensis* H.S.Yoon & R.A.Andersen
	**S. caribensis* H.S.Yoon & R.A.Andersen
	**S. kuepperi* R.A.Andersen & B.Melkonian
FAMILY Sarcinochrysidaceae (11 genera, 15 species)	
	**Andersenia australica* R.Wetherbee & R.F.Waller
	**A. nodulosa* R.Wetherbee & R.F.Waller
	**Arachnochrysis demoulinii* R.A.Andersen & K.Y.Han
	**Aureoscheda bahamensis* M.J.Wynne & R.A.Andersen
	**Aureoumbra lagunensis* D.A.Stockwell, DeYoe, Hargraves & P.W.Johnson
	**A. geitleri* M.Melkonian & C.P.Reyes
	Chrysonephos lewisii (W.R.Taylor) W.R.Taylor
	**Gazia saundersii* Wetherbee & Bringloe
	**G. australia* Wetherbee & Bringloe
	**Glomerochrysis psammophila* Wetherbee
	Nematochrysopsis marina (J.Feldmann) C.Billard
	**Pelagospilus aureus* R.A.Andersen & L.Graf
	**Sarcinochrysis marina* L.Geitler
	**Sargassococcus epiphyticus* R.A.Andersen & M.Melkonian
	**S. simulans* R.A.Andersen & M.Melkonian
ORDER Pelagomonadales R.A.Andersen & G.W.Saunders (with 1 family)	
FAMILY Pelagomonadaceae R.A.Andersen & G.W.Saunders (with 7 genera, 7 species)	
	**Ankylochrysis lutea* (van der Veer) C.Billard
	**Aureococcus anophagefferens* Hargraves & Sieburth
	**Chromopallida australis* Wetherbee
	**Chrysophaeum taylorii* I.F.Lewis & H.F.Bryan
	**Pelagococcus subviridis* R.E.Norris
	**Pelagomonas calceolata* R.A.Andersen & G.Saunders
	**Wyeophycus julieharrissiae* Wetherbee
ORDER Plocamiomonadales Daugbjerg & Lovejoy ord. nov. (with 1 family)	
FAMILY Plocamiomonadaceae Daugbjerg & Lovejoy fam. nov. (with 1 genus, 1 species)	
	**Plocamiomonas psychrophila* Daugbjerg & Lovejoy gen. et sp. nov.
Incertae sedis	
	Sulcochrysis biplastida D.Honda, M.Kawachi & Inouye

Species marked with an * have been sequenced for nuclear-encoded SSU rRNA.
Nematochrysopsis marina is tentatively placed in the Sarcinochrysidaceae until a DNA sequence-based taxonomy becomes available. Note that Gayral & Billard (1986) placed it in a family of its own, Nematochrysopsidaceae.

120–140 nm in *Wyeophycus julieharrissiae* (Wetherbee *et al.*, 2023). Depending on the pelagophyte species, cells were surrounded by 2–5 layers except where the flagellum/flagella emerge in flagellate or zoospore stages. Note that *Pelagomonas calceolata* may only have one layer (Wetherbee *et al.*, 2023). Layers 2 and 4 were electron dense and perforated by up to two types of pores differing in diameter. Therefore, the theca was termed a perforated theca (PT) (Wetherbee *et al.*, 2021). These pores, with a size range of 5–25 nm in diameter, are very difficult to see using standard fixation protocols (own observations). Layer 1, which is present in all species and layers 3 and 5 (if present) stained only slightly and comprised either fibres or fibrillar protrusions. Thus, the perforated theca is the synapomorphic character and the number of layers (1–5) the character state. See Wetherbee *et al.* (2023) for further details on thecal layers. Layers should be counted from the plasma membrane and the terminology suggested by Wetherbee *et al.* (2023) was followed here.

All pelagophytes currently described are marine and they are present in all climate zones. Some species have a wide biogeographic distribution (e.g. *Pelagomonas calceolata* (www.gbif.org/species/3195486), *Pelagococcus subviridis* (www.gbif.org/species/3195489), *Aureococcus anophagefferens* (www.gbif.org/species/3195491), *Ankylochrysis lutea* (www.gbif.org/species/3195300) and *Aureoumbra lagunensis* (www.gbif.org/species/3195308) [all data accessed 5 May 2024]) whereas others are restricted in their distribution. For example, the recently described genera *Wyeophycus, Gazia, Andersenia* and *Chromopallida* are currently only known from southeastern Australia (including Tasmania) (Wetherbee *et al.*, 2015, 2021, 2023). Another genus *Pituiglomerulus* is only known from eastern Australia (Wetherbee *et al.*, 2023) and *Glomerochrysis* only from western Australia (Wetherbee *et al.*, 2021). A few pelagophytes are known from the Caribbean Sea (*Sungminbooa caribensis* and *Aureoscheda bahamensis*) and the Sargasso

Sea (*Sargassococcus epiphyticus* and *S. simulans*) (Han *et al.*, 2018). In European waters *Arachnochrysis demoulinii* occurs in the Mediterranean Sea (Corsica) and *Aureoumbra geitleri* near Gran Canaria (Canary Islands) (Han *et al.*, 2018).

Pelagophytes are autotrophic members of the Heterokontophyta having at least in the flagellate or zoospore stage, 1 or 2 chloroplasts with three adpressed thylakoids surrounded by a girdle lamella, bipartite (no lateral filaments) or tripartite flagellar hairs (mastigonemes). Most vegetative stages are filamentous or form cell colonies (clusters, clouds, cubes) and possess 1–2 chloroplasts per cell (Han *et al.*, 2018). However, *Chrysocystis* spp. and *Chrysoreinhardia algicola* differ from this pattern by having four or eight chloroplasts per cell (Han *et al.*, 2018). With respect to the cellular organization pelagophytes are highly diverse, as species in the Pelagomonadales are either flagellates or coccoids, whereas the Sarcinochrysidales are either benthic palmelloids, filaments or colonies. The major photosynthetic accessory pigments are fucoxanthin, diatoxanthin, diadinoxanthin, and sometimes 19'-butanoxylofucoxanthin.

Molecular phylogenetic studies of the Heterokontophyta based on single (Cavalier-Smith & Chao, 2006) or multi-gene analyses (Riisberg *et al.*, 2009; Han *et al.*, 2018) all favoured a sister group relationship between Pelagophyceae and Dictyochophyceae. This relationship has received systematic significance as Cavalier-Smith & Chao (2006) proposed the subclass Alophycidae for the evolutionary lineage. Recently a phylogenetic analysis using 120 genes revealed bolidophytes and diatoms as the sister group to the Alophycidae (Thakur *et al.*, 2019). Thus, the phylogeny and evolutionary history of the Pelagophyceae seems well accounted for. Also, the habitat in which to observe pelagophytes is diverse being either planktonic (e.g. *Pelagomonas calceolata, Pelagococcus subviridis* and *Chromopallida australis*), epiphytic (e.g. *Sargassococcus epiphyticus*) or benthic (e.g. *Arachnochrysis demoulinii, Wyeophycus julieharrissiae* and *Pituiglomerulus capricornicus*).

Collectively the morphology, phylogeny and collection site of the strain described here as a new pelagophyte taxon expanded not only our understanding of biogeography and habitat range of the group but also the current classification at the order and family level. Observations using light and transmission electron microscopy using a standard fixation protocol, showed several novel morphological features for the Pelagophyceae. The three most important were (1) a thin filament connecting the central axonemes to a short central electron-dense thickening above the transitional plate in the flagellar transition region; (2) a swelling on the mature flagellum consisting of one or two enlargements with different thicknesses; and (3) non-microtubule supported arm-like structures extending from the cell surface. To document the ecological status of *P. psychrophila* as a cold-water species we conducted a series of autecological temperature experiments. The results of this study (and the growth rate tolerance to changes in salinity and pH values) were given in Supplementary document S1. However, summaries of the main results are provided herein.

Materials and methods

Sampling and culture conditions

The autotrophic nanoflagellate studied here was collected on 15 June 1998 from a small ice melt hole or pocket that remained unfrozen and presumably in contact with ice brine channels but not with the ocean below, in the northern part of Baffin Bay, Canadian Arctic (Supplementary fig. S1) (Hamilton *et al.*, 2008; Freyria *et al.*, 2022). A unialgal culture was established by CL via progressive selection and three years later it was deposited at the National Center for Marine Algae and Microbiota (NCMA, formerly CCMP) as CCMP2097. A duplicate culture has been kept at Marine Biological Section, University of Copenhagen, under the strain name YellowSIPH for more than 23 years. This study was based on the material grown in Denmark under a temperature of 4°C, in L1 growth medium (without Si) (Guillard & Hargraves, 1993) with a salinity of 30 and a 16:8 h light:dark cycle. The light intensity was 80–100 µmol photons m^{-2} s^{-1} (except for material used for confocal microscopy, see below).

Light microscopy

Live cells were studied using a Zeiss Axio Imager M2 light microscope (Carl Zeiss, Göttingen, Germany) equipped with differential interference contrast optics and a 63× Plan Apochromat oil immersion objective lens. Colour micrographs were taken with a Zeiss AxioCam HRc digital camera. Micrographs of chloroplast autofluorescence were recorded with a Zeiss Axiocam 506 mono digital camera and live cells were excited with the filter set 09 from Zeiss (excitation band pass 450–490 and emission 585 long pass).

Confocal microscopy

The CCMP2097 culture was grown in L1 (without Si) media containing antibiotics (penicillin 5 U ml^{-1}, neomycin 10 µg ml^{-1}, streptomycin 5 µg ml^{-1}) at 4°C and with a light intensity of 8.3 µmol photons m^{-2} s^{-1} in a Percival Algae growth chamber. Cells were collected at

the end of the exponential growth phase and fixed in paraformaldehyde (final concentration 0.1%) and glutaraldehyde (final concentration 1%). 20 µl of fixed culture containing 10 µg ml^{-1} DAPI was placed on Fisherbrand™ Superfrost™ Plus Microscope slides and set at room temperature in the dark for 30 min. Adhered cells were gently rinsed with 0.2 µm filtered Milli-Q water. The rinsed microscope slide was dried at room temperature, until the last trace of water disappeared. Microscope slide preparation was completed by covering the sample with #1.5 coverslip containing 20–30 µl of Zeiss 518 N immersion oil and sealed with nail polish. Confocal imaging was performed with an SP8 Leica confocal microscope using a 63× objective lens. Red fluorescence (737–779 nm) was excited with the 488 nm laser and detected with hybrid detectors. Adaptative fluorescence deconvolution (lightning) was applied on the z-stack and 3D reconstitution was performed with the LasX software.

Transmission electron microscopy

Whole mounts were prepared as outlined in Moestrup and Thomsen (1980) but instead of shadow-casting the material it was stained in 2% aqueous uranyl acetate as described in Daugbjerg & Moestrup (1992*a*). Thin-sectioned material was prepared as in Daugbjerg (1996). The material was examined in a JEOL JEM-1010 transmission electron microscope operated at 80 kV (JEOL Ltd, Tokyo, Japan) at Dept. of Biology, University of Copenhagen. Micrographs were taken using a Gatan Orius digital camera (Gatan Inc., Pleasanton, California, USA).

Pigment analyses

For HPLC non-water-soluble pigments were extracted in 95% methanol and separated with a Accela 600 HPLC system on a reverse-phase Hypersil Gold C-8 column. The solvent contained methanol, aqueous pyridine, acetone and acetonitrile (Zapata *et al.*, 2000). Chromatograms were recorded on an Accela PDA detector at 450 nm and pigment spectra over wavelengths ranging between 350–800 nm. A Finnigan Surveyor FL Plus fluorescence detector with an excitation of 440 nm and an emission of 650 nm (optimized for chlorophyll *a*) was also applied to identify and quantify chlorophyll pigments. The detector was calibrated by repeated injections of 30 pigment standards from Sigma Aldrich (MO, USA) and DHI (Denmark). ChromeQuest software was applied to identify and quantify the concentrations of pigments. The photodiode array spectrum of each peak was checked against the reference spectra of standards or against a reference spectrum used in Roy *et al.* (2011) for pigments for which a standard does not exist.

Phylogenetic inference

The nuclear-encoded SSU rRNA gene (1791 bp) of strain CCMP2097 was previously determined by Hamilton *et al.* (2008). As our aim was to infer the phylogeny of this strain as accurately as possible within the Pelagophyceae a BLASTn search in GenBank (latest 11 January 2024) was conducted. This revealed eight SSU rRNA sequences closely matching that of *Plocamiomonas psychrophila* (accession number EU247837). The similarities ranged between 98.51–100% identity and included 1659–1767 base pairs for the comparisons. All of these belonged to uncultured material from clone libraries for which no other gene sequences are available. Hence, we saw no merit in conducting a multigene phylogeny that included several chloroplast-encoded genes as that would have reduced the number of taxa contributing to the phylogenetic signal with specific reference to *P. psychrophila*. The SSU rRNA based alignment consisted of 51 pelagophyte taxa including *P. psychrophila* and of these 27 sequences of cultured material were identified to species (included 19 genera) and one sequence of cultured material was only identified to genus level (i.e. *Chrysocystis* sp. strain MBIC11134). Seventeen sequences represented uncultured pelagophytes and six were cultured but unidentified or likely incorrectly identified as with '*Chrysoreinhardia* sp.' (CCMP2950). The pelagophyte taxa were rooted using five diatom species (five genera). Three bolidophyte species belonging to the genus *Triparma* and six dictyochophyte sequences (five genera) were also included. The latter class has been shown to form a sister group to the Pelagophyceae (e.g. Ali *et al.*, 2002; Riisberg *et al.*, 2009; Yang *et al.*, 2012; Thakur *et al.*, 2019). Two approaches for phylogenetic reconstructions were applied: Bayesian analysis (BA) with MrBayes ver. 3.2.6 (Ronquist & Huelsenbeck, 2003) and PhyML ver. 3.3.2 (Guindon *et al.*, 2010) as implemented in Geneious Prime (ver. 2023.2.1). A general time-reversible substitution model with base frequencies and gamma substitution rate matrix estimated from the data was used for BA. It was run for 5 million Markov Chain Monte Carlo generations with four parallel chains. For every 1000th generation a tree was sampled, and the burn-in was set to 500 000. This left 4501 trees for estimating posterior probabilities. Thus, 500 trees were discarded, and posterior probability values were obtained from a 50% majority-rule consensus of the saved trees. For PhyML the GTR substitution model was used with 1000 bootstrap replications. Bootstrap support values >50% were mapped onto the tree obtained from BA.

Sequence divergence

The Kimura-2-parameter model available in PAUP* (ver. 4.0a, build 169; Swofford, 2002) was used to

estimate the sequence divergences between all pairwise comparisons of pelagophytes and between *Plocamiomonas* and selected pelagophytes.

Results

Taxonomy and nomenclature follows the International Code of Nomenclature for algae, fungi and plants.

Plocamiomonadales Daugbjerg and Lovejoy, ord. nov.

DIAGNOSIS: With characteristics of the family.

Plocamiomonadaceae Daugbjerg and Lovejoy, fam. nov.

DIAGNOSIS: Biflagellated cells possessing microtubular (=kinetosomal) roots. Swelling on mature flagellum and transitional plate in transition zone. 19'-butanoyloxyfucoxanthin and diadinoxanthin present. No gel matrix around cells.

Plocamiomonas Daugbjerg and Lovejoy, gen. nov.

DIAGNOSIS: Lateral insertion of flagella. Cells surrounded by bi-layered theca. Non-microtubule supported arm-like structures extend from cell surface. Chloroplast with embedded pyrenoid traversed by thylakoids. Peripheral vesicles. Characterized by unique DNA sequence representing nuclear-encoded SSU rRNA.
TYPE SPECIES: *Plocamiomonas psychrophila* Daugbjerg & Lovejoy.
ETYMOLOGY: from 'plocamos' (Gr.) lock of hair; and 'monas' (Gr.) unit (monad).

Plocamiomonas psychrophila Daugbjerg & Lovejoy, sp. nov. (Fig. 3)

DIAGNOSIS: Cells spherical, 5–11 µm in diameter. With a single peripheral, deeply lobed chloroplast, yellow brown in colour. Two lateral flagella slightly unequal in length (hairy flagellum longest), 1.5–2 times longer than the cell. A posterior nucleus lies close to the basal bodies (ventral side). In live material, extending arm-like structures are equal to or shorter than the cell in length. Thin filament connects the central pairs of microtubules to a central, narrow thickening in the flagellar transition region. No coccoid or cyst stages noted. DNA representing nuclear-encoded SSU rRNA (EU247837) distinctive and unique.
ETYMOLOGY: from 'psukhros' (Gr.) cold; and 'philos' (Gr.) loving.
HOLOTYPE: Thin-sectioned material of *Plocamiomonas psychrophila* (Yellow SIPH = CCMP2097) embedded in Epon has been deposited at the Botanical Museum, University of Copenhagen. This material serves as the designated type, and it was given the reference number C-A-99711.
TYPE LOCALITY: Small pocket of liquid water on the surface of the ice in Baffin Bay, North America (77.0014°N and 77.2383°W). See Supplementary fig. S1.
HABITAT: Marine.

Light and epifluorescence microscopy

The cell body was spherical and had a diameter of 7.5 µm ± 0.8 (max. cell diameter = 10.4 µm, min. cell diameter = 5.6 µm, n = 39) (Figs 1–6). Two flagella slightly unequal in length emerged from the lateral side as defined from the swimming direction (Figs 2, 4). They were 1.5–2 times longer than the cell diameter. The immature flagellum pointed forward and was beating with the typical sinusoidal pattern whereas the backward pointed mature flagellum had a stiffer sculling motion (Fig. 1). In non-swimming cells the flagella were positioned in more or less the same direction (Figs 2, 3). The single peripheral chloroplast was yellow brown and in epifluorescence microscopy observed to be deeply lobed (Figs 7, 8). A super resolution 3D reconstruction ('lightning technique') of the chloroplast was shown as Supplementary fig. S2. Here the chloroplast was also seen to form two deep lobes. A large vacuole probably containing chrysolaminaran was discerned in many cells (Figs 5, 6, 9). Some cells possessed large numbers of arm-like structures extending from the cell surface (Figs 4, 10, 11). The majority of these were shorter than the cell (Fig. 11) but a few were similar to the cell diameter (Figs 4, 10). The arm-like structures were particularly easy to observe in phase contrast (Figs 10, 11). Numerous peripheral vesicles were also noted (Figs. 1, 4). Coccoid stages and resting cysts were not observed.

Swimming behaviour

Cells swam in a straight path while rotating around their longitudinal axis. The forward-directed flagellum showed the typical sinusoidal movement for heterokont algae. The second flagellum was trailing and due to its length, it could be seen behind the cell.

Transmission electron microscopy

The general disposition of cell organelles was shown in Figs 12, 13. The peripheral vesicles seen in the light microscope were also discernible in electron

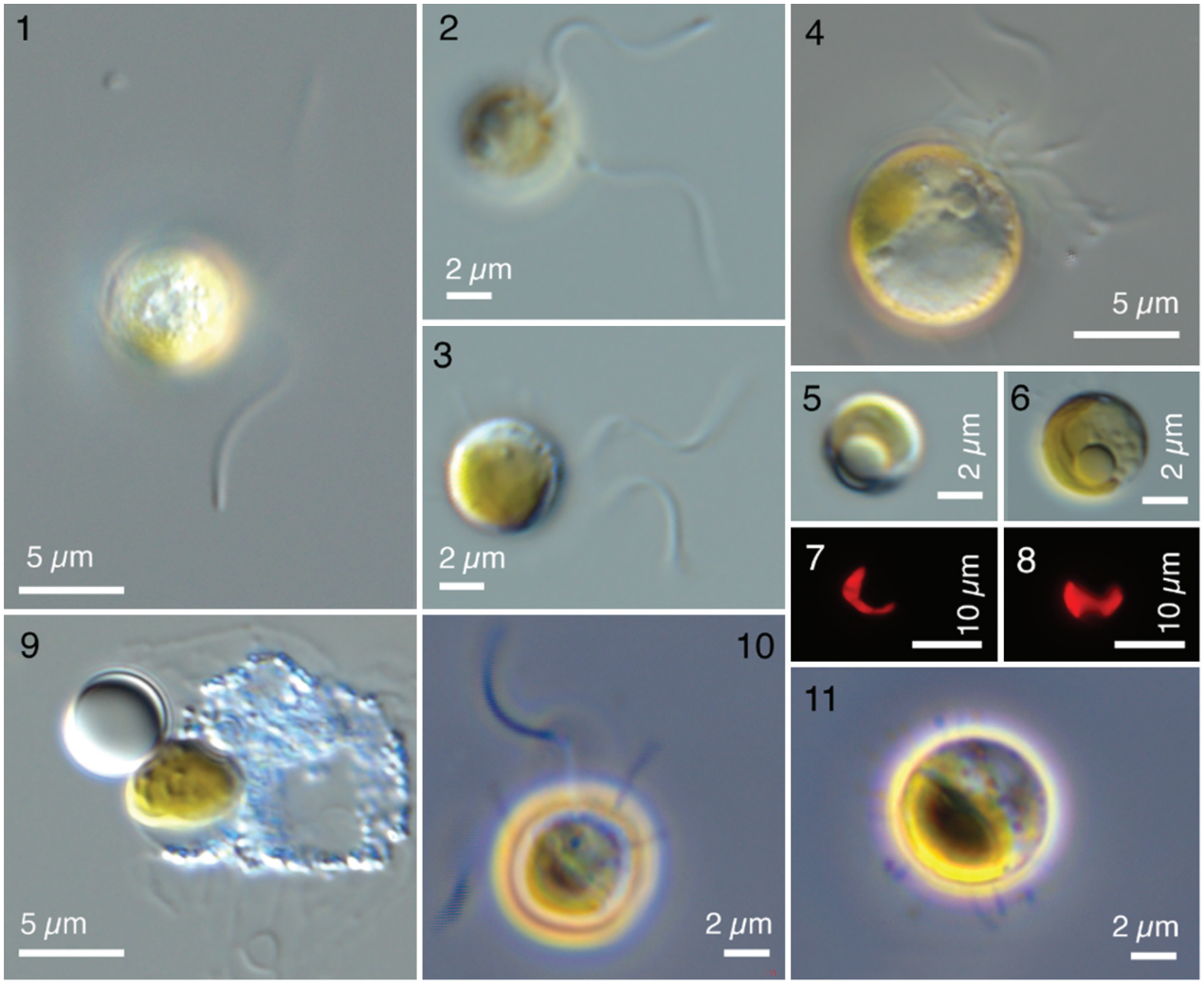

Figs 1–11. Light micrographs of *Plocamiomonas psychrophila* gen. et sp. nov. Nomarski interference contrast (**Figs 1–6, 9**), epifluorescence microscopy (**Figs 7, 8**) and phase contrast (**Figs 10, 11**). **Fig. 1**. Surface view showing numerous peripheral vesicles. The laterally inserted flagella point in opposite directions. The immature flagellum directed forward, and mature flagellum pointed backwards. **Figs 2, 3**. Cells at rest with flagella pointing in the same direction. **Fig. 4**. Cell with extending arm-like structures in the flagellar insertion area. **Figs 5, 6**. Cells with vesicles perhaps containing chrysolaminaran. The lobed chloroplast can be discerned in **Fig. 6. Figs 7, 8**. Chloroplast autofluorescence. Note deeply lobed chloroplast in **Fig. 7. Fig. 9**. Exploded cell revealing single chloroplast and chrysolaminaran? vesicle. **Figs 10, 11**. Cells with extending arm-like structures of different length covering parts of cell surface. Two flagella can be seen in **Fig. 10**.

microscopy as differently sized, membrane-bound vesicles scattered in the cell perimeter (Figs 12, 13). Larger magnifications of the membrane-bound vesicles were shown in Figs 14, 16. Most vesicles appeared empty, but a few contained slightly stained fibrillar material. The chloroplast was peripheral (Fig. 12), and the section shown in Fig. 13 supported the presence of two lobes. A pyrenoid matrix was embedded in one of the chloroplast lobes (Figs. 12, 13) and traversed by a few paired thylakoid lamellae (Fig. 15). The thylakoids were arranged in adpressed stacks of 3 and surrounded by a girdle lamella (Fig. 14) as typical for members of the Heterokontophyta. The nucleus with its nucleolus was large and took up a major part (Figs 12, 13) of the posterior-ventral part of the cell (Figs 33, 34). A few mitochondrial profiles were evident in most sections (Figs 12, 13). However, it was not determined if they formed a reticular network as seen in *Ankylochrysis lutea* (Honda & Inouye, 1995). A bilayered theca (20.7 ± 4.5 nm in thickness; n = 24) was seen to adjoin the plasma membrane and thus cover the whole cell (Figs 12–16). Layer 1 measured 9.3 ± 2.4 nm in thickness (n = 24) and did not stain well. The thickness of layer 2 was 11.4 ± 2.2 nm (n = 24) and it was electron dense. The fixation schedule used here (not based on high-pressure freezing) did not allow for detailed observations of the pores likely present in layer 2. Consequently, we could not determine if two types of pores with a different diameter were part of this thecal layer as has been shown for *Wyeophycus julieharrissiae, Ankylochrysis lutea* and *Gazia australica* (Wetherbee *et al*., 2023).

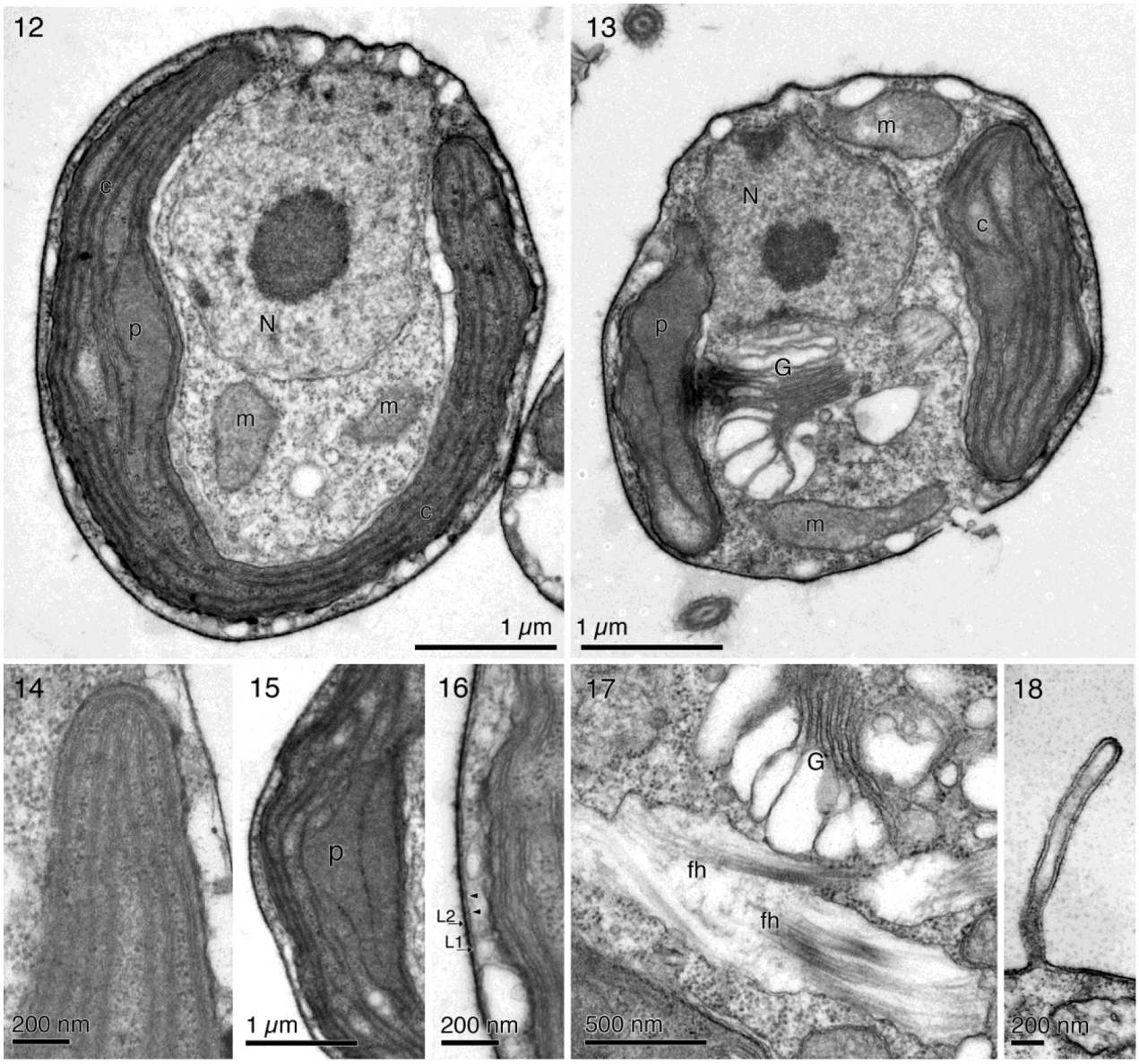

Figs 12–18. Transmission electron microscopy of *Plocamiomonas psychrophila* gen. et sp. nov. **Figs 12, 13**. Sections showing disposition of major cell organelles (N = nucleus, c = chloroplast, m = mitochondrion, p = pyrenoid, G = Golgi body). Note deeply lobed chloroplast in **Fig. 12. Fig. 14**. Details of chloroplast with thylakoids arranged in stacks of three and chloroplast matrix surrounded by a girdle lamella. **Fig. 15**. Details of pyrenoid (p) traversed by a few pairs of thylakoids. **Fig. 16**. Details of bi-layered theca (L1 = layer 1, L2 = layer 2) and the plasma membrane underneath (arrowheads). **Fig. 17**. Bundles of flagella hairs (fh) inside vacuole next to the Golgi body (G). **Fig. 18**. Longitudinal section of arm-like structure extending from cell surface and enclosed by bi-layered theca. Plasma membrane also appeared to extend the full length of the arm-like structure. Tubular part of arm-like structure contained electron-dense material.

Bundles of flagellar hairs (mastigonemes) were located in a vacuole adjacent to the Golgi body (Fig. 17). The protruding arm-like structures seen in the light microscope were on a few occasions also noticed in thin-sectioned material. The protruding arm-like structure shown in Fig. 18 was 1.5 μm long and 0.14 μm wide, thus shorter compared with the length in live material. The plasma membrane seemed to extend into the arm as did layers 1 and 2 (Fig. 18). Cytoplasmic material filled up the projection (seen as electron-dense material). In material prepared for whole mounts the arm-like structures extending from the cell surface were seen in some cells (Fig. 20) but not in others (Fig. 19).

Flagella and flagellar transition zone

Some variation was noted with respect to the flagellar hair tip shown at high magnification in Fig. 21. In some cells both flagella possessed a hair tip (Fig. 19) whereas in other cells only the mature flagellum possessed this feature (Fig. 20). Variation was also noted in the length of the hair point, as it varied between 1 and 2.3 μm (Figs 19, 20). It remains to be determined if the hair tip has any significance or if

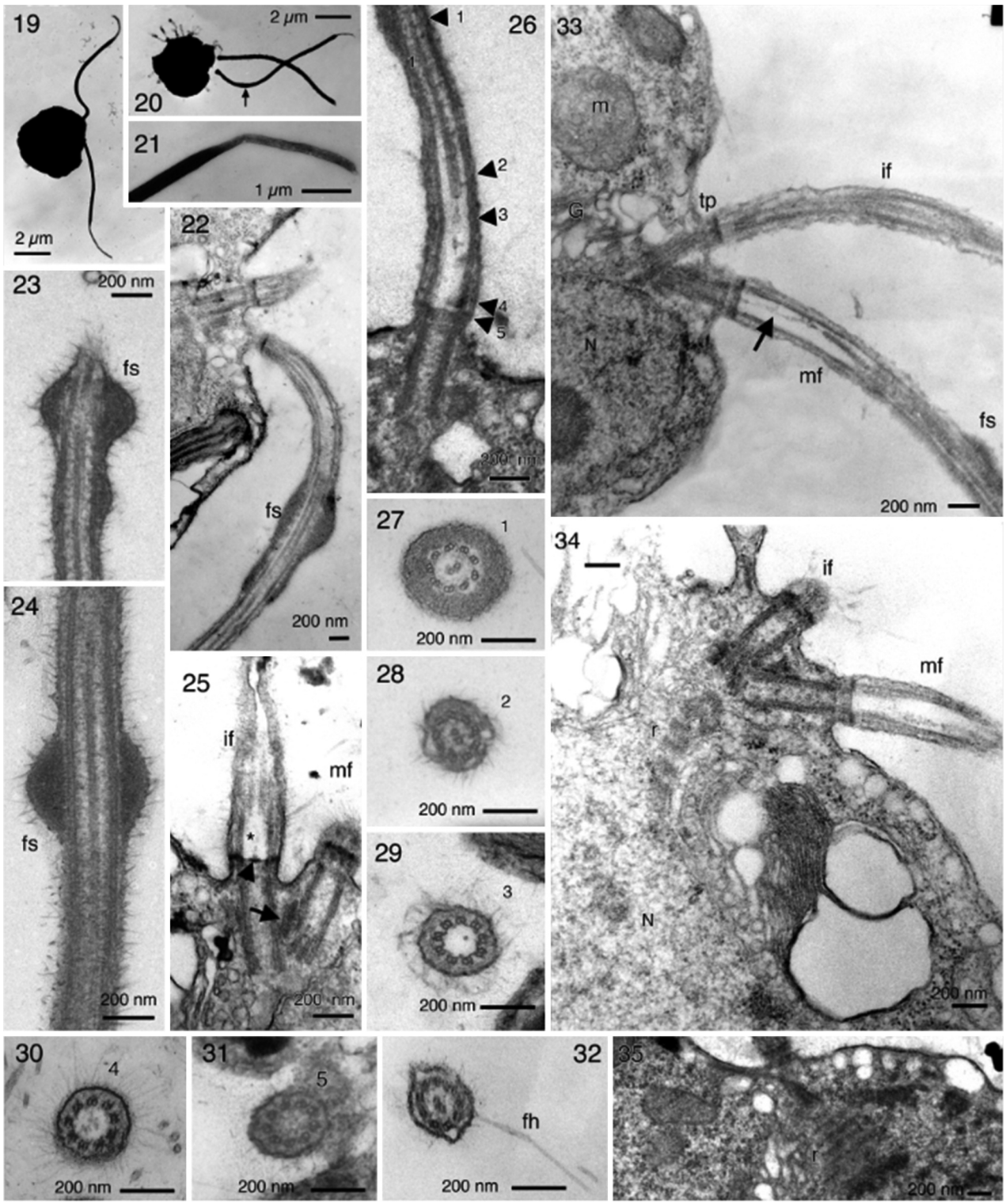

Figs 19–35. Transmission electron microscopy of *Plocamiomonas psychrophila* gen. et sp. nov., illustrating flagellar features and the mid-ventral part of cells. **Figs 19, 20**. Whole mount preparations showing cells with two almost equally long flagella. Note hair tip on one flagellum in **Fig. 20** and on both flagella in **Fig. 19**. Numerous arm-like structures extend from cell surface in **Fig. 20** but not in **Fig. 19**. Flagellar swelling may also be discerned in Fig. 20 (arrow). **Fig. 21**. Distal part of flagellum with hair tip. **Fig. 22**. Longitudinal section through mid-ventral end showing mature flagellum with flagellar swelling (fs). **Figs 23, 24**. Longitudinal sections through flagellar swelling (fs). Note double swelling in **Fig. 23** and single swelling in **Fig. 24. Fig. 25**. Longitudinal section through proximal part of immature (im) and mature (mf) flagella. Note central thickening of the transitional plate (arrowhead). One of the flagellar roots could be seen between the basal bodies (arrow). The thin filament between central axonemes and the transitional plate was indicated by an asterisk (*). Transitional plate also presents in mature flagellum. **Fig. 26**. Longitudinal section through flagellum/basal body. Numbered arrowheads 1–5 indicated the level of transverse sections through the flagellum in **Figs 27–31. Fig. 27**. Section through the flagellar swelling on the mature flagellum, with 9 × 2 + 2 axonemal arrangement of microtubules. **Fig. 28**. Section through the typical 9 × 2 + 2 microtubular arrangement typical of flagella in eukaryotes. **Fig. 29**. Section through the proximal part of the flagellum. Notice thin filament replacing the central microtubules. **Fig. 30**. Section at the level of tufts of 'hair-like' structures. **Fig. 31**. Cross section near transitional plate. **Fig. 32**. Cross section through flagellum with one flagellar hair (fh) (= mastigoneme).

it was an artefact of fixation. The mature flagellum possessed a swelling, seen as an electron-dense enlargement up to 1.2 µm in length (Figs 22–24). In longitudinal sections the swelling consisted of two interconnected enlargements differing in thickness (460 versus 285 nm, Fig. 23). In another longitudinal section the flagellar swelling was observed to consist of only a single enlargement (Fig. 24). Hence, some variation was noted with respect to the morphology of the swelling.

The flagellar transition zone was shown in several longitudinal sections (Figs 22, 25, 33, 34). The single transitional plate marks the transition from flagellum to basal body. In the proximal part of the flagellum the two central microtubules were replaced by a thin filament, approximately 500–600 nm in length and 30 nm in thickness. This structure attached to a central, narrow thickening in the transitional plate (Fig. 25). A transitional helix below the transition plate was not observed. A schematic drawing of the flagellar transition zone in longitudinal section was shown as Fig. 36. Six transverse sections marked in Fig. 26 were included as Figs 27–32 to illustrate fine structural variation at different levels of the flagella. Some of these are briefly commented on here. A cross section through the flagellar swelling where it had a medium diameter (380 nm) was shown in Fig. 27. The thin filament replacing the central axonemal microtubule was illustrated in Fig. 29, whereas the other cross sections shown in Figs 28, 32 were more representative of heterokonts, e.g. the 9 × 2 + 2 axonemal arrangement of microtubules and the 9 × 3 microtubules in the basal body.

Flagellar apparatus

The three-dimensional configuration of the flagellar apparatus was not determined but a few details were provided. The angle between the basal bodies was 30–45° (Figs 25, 33, 34) and their proximal part adjoined the nucleus and Golgi body in the ventral part of the cell (Fig. 34). Flagellar roots were seen in thin-sectioned material but the number of microtubules of individual roots and their path remained to be elucidated. Flagellar roots were discerned in Figs 25, 34. A striated fibrous root (= rhizoplast, system II fibre(s)) was present below the basal bodies. It extended towards the posterior end and close to the nucleus (Figs 34, 35), but the exact end point was not established.

Pigment composition

Analysis of photosynthetic pigments revealed the presence of chlorophyll *a* and c_2 in addition to the carotenoids β,β-carotene, fucoxanthin, 19'-butanoyloxyfucoxanthin and diadinoxanthin (data not shown). The concentration ratio between fucoxanthin and 19'-butanoyloxyfucoxanthin was 50:1 and between fucoxanthin and diadinoxanthin it was 4:1 (data not shown).

Molecular phylogeny

The single gene phylogeny based on nuclear-encoded SSU rRNA is shown in Fig. 37. Using five diatom genera (Bacillariophyceae) as outgroup taxa, the Pelagophyceae formed a monophyletic group highly supported by posterior probabilities (PP = 1.0) and bootstrap values (BS = 100%). The Dictyochophyceae which also formed a highly supported monophyletic group was the sister to the pelagophytes. The Bolidophyceae formed a sister group to the Pelagophyceae and Dictyochophyceae. Hence, the highly supported branching pattern for these classes of Heterokontophyta was similar to that based on concatenated phylogenetic analyses (Yang *et al.*, 2012; Thakur *et al.*, 2019). Phylogenetic analyses of SSU rRNA sequences also supported the currently accepted taxonomy of orders within the Dictyochophyceae as the Dictyocales, Florenciellales and Pedinellales all formed highly supported monophyletic lineages. With respect to the Pelagophyceae, the tree topology revealed four highly to moderately supported clades that echoed the two families within the Sarcinochrysidales (PP = 1.0 and BS = 98%) (Sarcinochrysidaceae with PP = 1.0 and BS = 99% and Chrysocystaceae with PP = 1.0 and BS = 89%), the Pelagomonadales (PP = 0.79 and BS < 50%) and finally a lineage comprising *Plocamiomonas* and eight uncultured pelagophyte clones from cold water (PP = 1.0 and BS = 97%). The origin of these was added to Fig. 37 and this lineage formed a sister group to Pelagomonadales and Sarcinochrysidales. However, the relationship was poorly supported (PP = 0.55 and BS < 50%). A fifth poorly supported

Fig. 33. Longitudinal section through the mid-ventral part of cell, showing swelling (fs) on mature flagellum (mf), immature flagellum (if), transitional plate (tp), thin filament inside the proximal part of the flagella (arrow). Some organelles are also shown (nucleus = N, Golgi body = g, mitochondrion = m). **Fig. 34**. Longitudinal section showing system II fibre (rhizoplast, r) positioned at the base of the basal bodies and continuing parallel to the nucleus (N). **Fig. 35**. Longitudinal section through system II fibre (rhizoplast, r) showing striations.

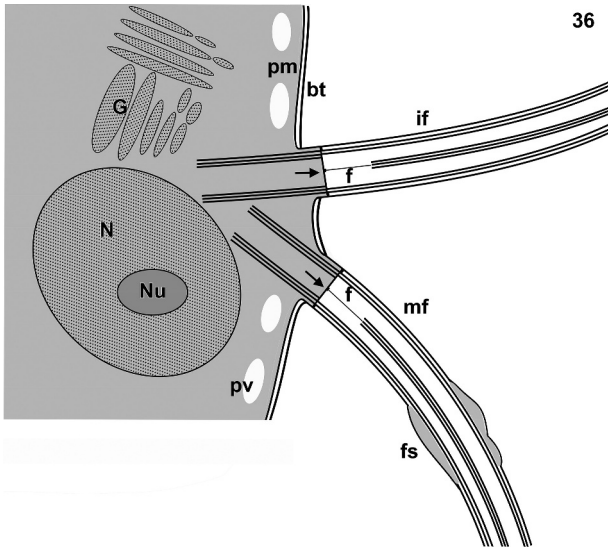

Fig. 36. Schematic drawing illustrating flagellar transition region in the mid-ventral part of *Plocamiomonas psychrophila* gen. et sp. nov. Flagellar roots and rhizoplast omitted. arrow = transitional plate with central thickening, bt = bi-layered theca, f = thin filament, fs = flagellar swelling, G = Golgi body, if = immature flagellum, mf = mature flagellum, N = nucleus, Nu = nucleolus, pv = peripheral vesicle, pm = plasma membrane. Not to scale.

lineage included another five uncultured pelagophytes (PP = 0.6 and BS = 56%). Their taxonomic affinity is yet unknown and the lineage therefore marked with a question mark in Fig. 37. Unfortunately, the sampling site(s) and depths for clones labelled 'NY13S' was not added to the GenBank accession files but are labelled following a convention for the North Yellow Sea, which is a shelf sea between China and the Korean peninsula (Zhu *et al.*, 2022). With respect to the species of interest here *Plocamiomonas psychrophila* formed a sister taxon to an uncultured pelagophyte clone from the Beaufort Sea with GenBank accession number JF698781. This relationship was well supported (PP = 1.0 and BS = 84%).

Sequence divergence

Plocamiomonas differed by 0.44% to the uncultured pelagophycean from Beaufort Sea (1630 base pairs included in the comparison). The five uncultured pelagophycean clones from the Gulf of Finland had an estimated sequence divergence ranging from 0.06–2.6% and they differed by 0.2–2.7% to *Plocamiomonas* (data not shown). The two uncultured clones from Svalbard differed by 1.6–1.8% when compared with *Plocamiomonas*. Comparing the sequence divergence for the five NY13S-clones and *Plocamiomonas* the sequence divergence ranged between 1.4–2.5%. For reasons of comparison the sequence divergence was also estimated between all members of the Pelagomonadales. Here the min. and max. values ranged between 0.062 and 6.6% (data not shown). It was noted that *Pelagomonas calceolata* and the coccoid pelagophycean CCMP1145 had identical SSU rRNA sequences and therefore this pairwise comparison was not included in the ranges provided.

Autecology

Variations in growth rates (cell divisions d^{-1}) of *Plocamiomonas psychrophila* strain CCMP2097 to changes in abiotic factors (salinity, temperature and pH) were studied in a series of autecological experiments. These were based on precise control (± 0.1°C) of pre-set temperatures using a custom-made relay system. See Supplementary document S1 for details on experimental setup, treatments and results. A summary of the main findings is provided here. The salinity experiment revealed that *Plocamiomonas* grew equally well at salinities ranging from 5–25 (in steps of 5) but significantly lower at a salinity of 30 (Supplementary fig. S9). It did not grow at a salinity of 0. The highest growth rate 0.63 d^{-1} was obtained at a salinity of 10 and the lowest 0.43 d^{-1} at a salinity of 30 (Supplementary fig. S9). The temperature (two treatments) and pH (three treatments) experiments were combined. With respect to temperature *Plocamiomonas* had a significantly higher growth rate at 3.8°C (average growth rate 0.52 d^{-1}) compared with 6.7°C (average growth rate 0.27 d^{-1}) (Supplementary fig. S11). The pH experiment with treatments at pH values of 8.1, 7.7 and 7.3 showed that temperature-dependent growth rates were intolerant to differences in pH levels (Supplementary fig. S11).

Discussion

Biogeography

With *Plocamiomonas psychrophila* our understanding of the biogeographic distribution of morphologically characterized pelagophyceans has expanded to include cold-water ecosystems and not just temperate and subtropical/tropical waters where all other members occur. Interestingly, the SSU rRNA sequence of *Plocamiomonas* was 100% identical to WS073-076, an uncultured, cloned sequence (1713 bp, GenBank accession number KP404824) from the South China Sea determined by Wu *et al.* (2015). In early September 2007, sea surface temperatures in the South China Sea ranged from 28.5–30°C and the lowest temperature for any of the sampled depths (50 m at Y93D) was 21°C (W. Wu, pers. comm.). Hence, future morphological and physiological studies of ribotype WS073.76 need to confirm the presence of *Plocamiomonas* in the China Sea. Until then we consider *Plocamiomonas psychrophila* a true cold-water species, which would be consistent with the high copy numbers of genes coding for ice-binding

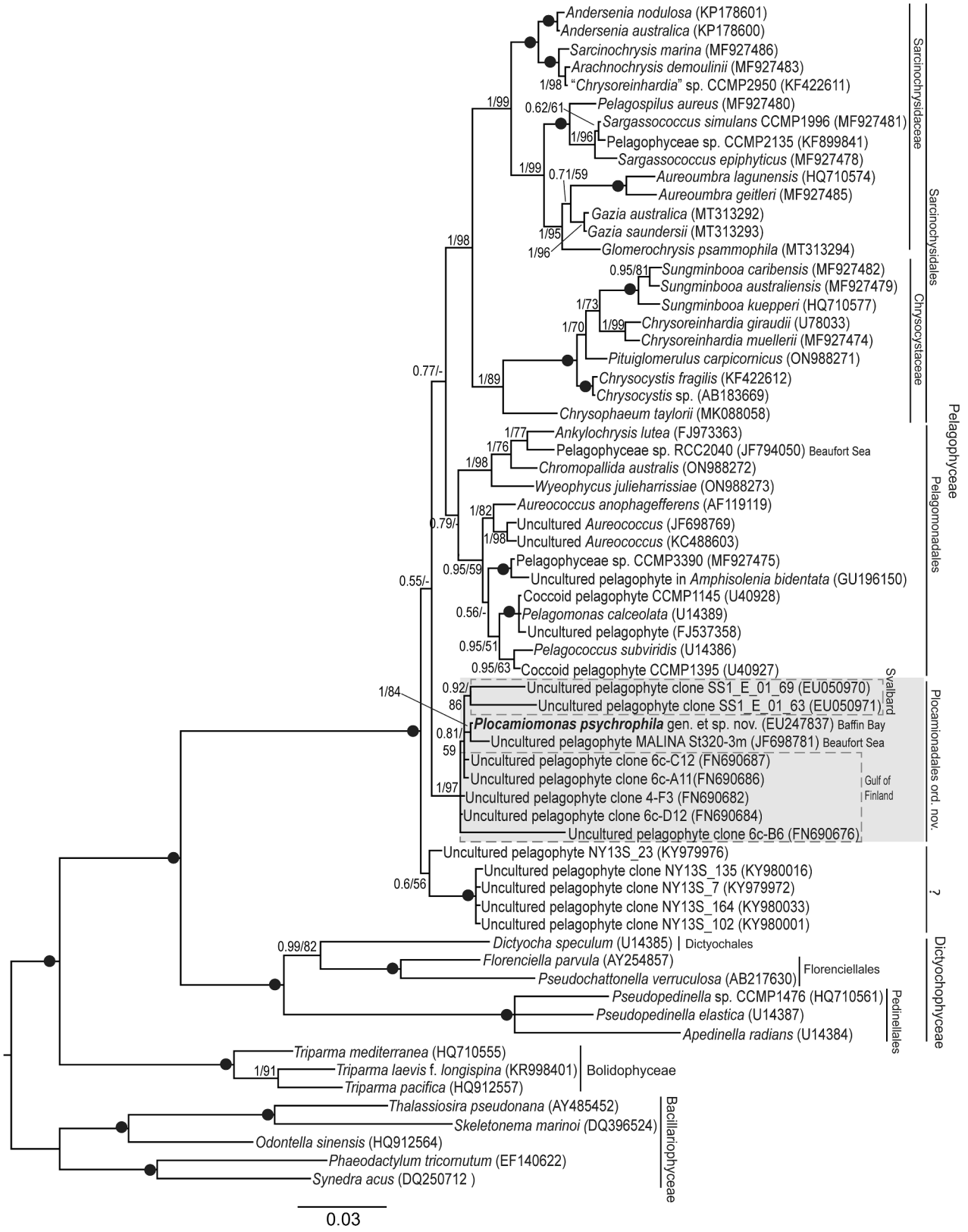

Fig. 37. Molecular phylogeny of *Plocamiomonas psychrophila* gen. et sp. nov. and 64 other Heterokontophyta inferred from Bayesian analysis (BA) of the nuclear-encoded SSU rRNA sequences. The aligned data matrix consisted of 1671 base pairs including introduced alignment gaps. Five diatoms (three centric and two pennate species) were used as outgroup taxa. Besides a diverse assemblage of pelagophytes (51 sequences representing 20 different genera, 27 identified species and 24 unidentified taxa), three bolidophytes (*Triparma* spp.) and five genera of dictyochophytes also formed part of the ingroup. Posterior probabilities (≥ 0.5) from BA with 5 million generations and bootstrap support values (≥ 50%) from maximum likelihood analyses (ML) with 1000 replications were given at internodes. Filled circles were used to indicate the highest possible support in BA and ML (1.0 and 100%, respectively). The new order Plocamiomonadales was marked by a grey box and the current taxonomy of Pelagophyceae and Dictyochophyceae was indicated by vertical lines. GenBank accession numbers were given in parentheses and clonal names for all uncultured pelagophytes. The geographic origins of cold-water taxa were given for members of Plocamiomonadales. Branch lengths were drawn so that they appeared proportional to the number of changes per site. *Plocamiomonas psychrophila* was marked in bold face. ? = unclassified pelagophytes.

proteins in the isolate (Freyria *et al*., 2022) It should also be noted that since a cyst stage was not observed in our material, it seems unlikely that ribotype WS073.76 was obtained from cyst DNA.

Phylogenetic inference

The resolution power of the phylogeny based on nuclear-encoded SSU rRNA was not sufficient to unravel with confidence the sister group relationships between the deepest lineages of Pelagophyceae, equivalent to the systematic level of orders (Fig. 37). This contrasts with the multigene phylogeny recently published by Wetherbee *et al*. (2023: fig. 1) where they inferred the phylogeny of 29 pelagophyte taxa and obtained the highest possible support values for the branching pattern of the deepest lineages. Their data matrix comprised a nuclear-encoded gene (SSU rRNA) and five chloroplast-encoded genes. Considering that *Plocamiomonas* clustered with eight uncultured clones for which no chloroplast genes are available and that all of these formed a lineage separate from existing pelagophyte lineages, we may ask if analysis of a single gene will adequately reflect a reliable relationship of these taxa. A detailed comparison between the single gene tree (Fig. 37 based on SSU rRNA) and a multigene tree, for example Fig. 1 in Wetherbee *et al*. (2023) may provide an answer to this question. Hence, if they differ, the phylogenetic position of *Plocamiomonas* and the closely related cold-water taxa can probably not be inferred with confidence. If on the other hand, the tree topologies concur then we can likely trust the tree topology obtained from the single gene analysis. Such a comparison revealed two rather insignificant differences. Firstly, in the SSU rRNA tree, *Wyeophycus* formed a sister taxon to *Chromopallida* and *Ankylochrysis* whereas in the multigene phylogeny *Chromopallida* formed a sister taxon to *Wyeophycus* and *Ankylochrysis*. Secondly, in the SSU rRNA tree *Pelagospilus* and the two species of *Sargassococcus* formed a sister group to a lineage with *Glomerochrysis, Gazia* spp. and *Aureoumbra* spp. whereas in the multigene analyses *Pelagospilus* and *Sargassococcus* spp. clustered with *Arachnochrysis, Sarcinochrysis* and *Andersenia*. However, both these clusterings received low branching support in the multigene phylogeny (78 and 89%, respectively; Fig. 1 in Wetherbee *et al*., 2023) and the branching pattern was therefore not conclusive. Based on this we conclude that the phylogeny inferred from SSU rRNA likely reveals the correct branching for *Plocamiomonas* and the closely related uncultured cold-water clones.

Due to low statistical support the deepest pelagophyte branches were unresolved. However, the order Sarcinochrysidales received high support and the Pelagomonadales moderate support from posterior probabilities and bootstrap. In morphological terms these taxa are markedly distinct. Species within the Sarcinochrysidales are characterized by being either sarcinoid, capsoid, bi-flagellated (with four flagellar roots) or filamentous (Wetherbee *et al*., 2015; Han *et al*., 2018), whereas species within the Pelagomonadales are coccoids, uni- or bi-flagellates (Andersen *et al*., 1993; Wetherbee *et al*., 2023). The lineage comprising *Plocamiomonas psychrophila* and eight cold-water uncultured pelagophytes from Svalbard, the Gulf of Finland and the Beaufort Sea received high support. This evolutionary lineage suggests the presence of a group of pelagophytes currently restricted to waters characterized by low temperatures. This observation also extends the biogeography for the class Pelagophyceae, and future studies should reveal if the uncultured pelagophytes from the Beaufort Sea and the Gulf of Finland represent one or more new species of *Plocamiomonas* as indicated by the tree topology with short branch lengths between these OTUs and sequence divergence estimates. The ribotype from Beaufort Sea may have a different ecology being sampled in open water (3 m), but in a region with floating ice, whereas *Plocamiomonas* has rarely been observed in metabarcoding libraries from open water (Lovejoy, personal observations). Some of the OTUs with long branch lengths, e.g. the two uncultured pelagophytes from Svalbard may represent a new genus within the Plocamiomonadales. For this to be further explored we need to establish several cultures for phenotypic studies.

Due to low branch support the phylogenetic position of the five uncultured pelagophyte 'NY13S'-clones could not be determined (Fig. 37). The taxonomic and evolutionary significance of this evolutionary lineage also remains to be fully understood. However, the phylogenetic inference has indicated that they may represent yet another novel pelagophyte order. If that shows to be the case the diversity of the class expands even further.

Comparing morphological features of Plocamiomonas to other pelagophytes

The ultrastructure of strain CCMP2097 was studied using a standard protocol with glutaraldehyde and osmium tetroxide as fixatives. This allowed for a rather detailed understanding of cell organelles, flagella and some flagellar apparatus features (Figs 12–35). The ultrastructure of thecal layers, some with pores of different numbers and size classes and recently shown to be unique for pelagophytes (Wetherbee *et al*., 2021, 2023) could not be

Table 2. Nineteen morphological characters and their states scored for selected pelagophytes. '+' = present; '–' = absent; 'Veg'. = vegetative stage; 'Flag'. = flagellate.

Order	Plocamiomonadales	Pelagomonadales						Sarcinochrysidales								Incertae sedis
Family	Plocamiomonadaceae	Pelagomonadaceae						Chrysocystaceae			Sarcinochrysidaceae					
Species / Character	*Plocamiomonas psychrophila*[1]	*Pelagomonas calceolata*[2,14]	*Pelagococcus subviridis*[3,14]	*Aureococcus anophagefferens*[4,14]	*Ankylochrysis lutea*[5,14]	*Chromopallida australis*[14]	*Wyeophycus julieharrissiae*[14]	*Chrysocystis fragilis* (zoospore)[6]	*Chrysoreinhardia giraudii* (zoospore)[7,14]	*Andersenia australis* (zoospore)[8,14]	*Aureoumbra lagunensis*[9,14]	*Sarcinochrysis marina* (zoospore)[10]	*Pelagospilus aureus* (zoospore)[11]	*Glomerochrysis psammophila* (zoospore)[12,14]	*Gazia saundersii* (zoospore)[12,14]	*Sulcochrysis biplastida*[13]
Thecal layers	2	1?	4	4?	4	4	5	?	2	2	2	?	?	2	2	0? (naked)
Flagellar number	2	1	0	0	2	2	2	2	2	2	0	2	2	2	2	2
Flagellar insertion	Lateral	Posterior	NA	NA	Lateral	Sub-apical	Sub-apical	Lateral	Lateral	Lateral	NA	Lateral	Lateral	Subapical	Sub-apical	Apical
Posterior flagellum with hair point	+	–	NA	NA	+	?	?	–	?	?	NA	+	?	?	?	+
Flagellar roots	+	–	NA	NA	+	?	?	?	?	?	NA	?	?	?	?	+
Flagellar swelling	+	–	NA	NA	–	?	?	–	?	?	NA	?	?	?	?	+
Paraxonemal rod	–	+	NA	NA	–	?	?	–	?	?	–	?	?	?	?	–
Basal body number	2	1	0	0	2	2	2	2	?	?	2	2	2	2	2	2
Transitional plate(s) in transition region	+	+	NA	NA	+	?	?	?	?	?	–	?	+	?	?	+
Thin filament between central pair of micro-tubules and transitional plate	+	–	NA	NA	–	?	?	?	?	?	NA	?	–	?	?	–
Transitional helix in transition region	–	+	NA	NA	–	?	?	?	?	?	–	?	–	?	?	+
System II fibre(s) (rhizoplast)	+	–	NA	NA	+	?	?	?	?	?	–	?	?	?	?	–
Chloroplast number	1	1	1	1	1	1	1	1	1	2	1	2	1	1	1	2
Pyrenoid traversed by thylakoids (embedded/stalked)	+ (embedded)	–	–	+ (embedded)	+ (embedded)	+ (embedded)	+ (multiple) (embedded)	+ (stalked)	?	?	+ (stalked)	+ (stalked)	+ (stalked in veg. cell)	+ (stalked in veg.)	+ (stalked in veg.)	+ (stalked)
Pyrenoid traversed by thylakoids	+	NA	NA	+ (rarely traversed)	+	?	?	–	?	?	–	–	– (veg.)	?	?	–
Vegetative stage	Flag.	Flag.	Coccoid, short budding filaments	Coccoid	Flag.	Flag.	Flag.	Gelatinous colony	Gelatinous colony	Mucilaginous filaments	Coccoid	Gelatinous colony	Gelatinous single cells	Colony	Colony	Flag.
Angle between basal bodies	30–45°	NA	NA	NA	20–25°	?	?	?	?	?	90°	?	?	?	?	90°
Peripheral vesicles	+	–	–	–	–	+	+	+	+ (few)	+	+ (few)	?	+	?	+	–
Scale-like structure	–	–	–	–	+	?	?	+	?	?	–	?	?	?	–	–

NA, not applicable; ? = unknown. [1]Present study; [2]Andersen *et al.* (1993); [3]Lewin *et al.* (1977); [4]Sieburth *et al.* (1988); DeYoe *et al.* (1997); [5]Honda & Inouye (1995); [6]Lobban *et al.* (1995); [7]Han *et al.* (2018); [8]Wetherbee *et al.* (2015); [9]DeYoe *et al.* (1997);[10]Gayral (1972); Gayral & Billard (1986); Han *et al.* (2018); [11]Han *et al.* (2018); [12]Wetherbee *et al.* (2021); [13]Honda *et al.* (1995); [14]Wetherbee *et al.* (2023).

determined. The morphological comparison provided below was therefore based on features available from standard fixation protocols.

When combining the results of the morphological treatment and the phylogenetic inference, *Plocamiomonas* obviously did not fit into the presently suggested systematic treatment of the Pelagophyceae. Rather it possessed several distinct morphological characters and the strain studied here was described as a new species (*P. psychrophila*) in a new genus *Plocamiomonas* and referred to a new family and order (see Results). A list of 19 morphological characters and their character states were compiled in Table 2. This allowed a direct comparison between *Plocamiomonas* and 14 selected genera of Pelagophyceae and the incertae sedis *Sulcochrysis biplastida*. Based on this *Plocamiomonas* shared most character states with *Ankylochrysis lutea* (13 out of 19). However, a few character states differed markedly between these taxa, notable the lack of a flagellar swelling, peripheral vesicles and arm-like extensions, the presence of a scale-like structure and four thecal layers in *Ankylochrysis* (Honda & Inouye, 1995; Wetherbee *et al.*, 2023). *Plocamiomonas* also displayed some overlap in character states (10 of 19) with *Sulcochrysis biplastida*. The most significant being the flagellar swelling on the mature flagellum. However, they also differed in several distinct characters, e.g. place of flagellar insertion, angle between basal bodies and lack of peripheral vesicles, and system II fibres in *Sulcochrysis*. It may also be worth mentioning that in *Sulcochrysis* the pyrenoid (one in each of the two chloroplasts) was not traversed by thylakoids and that a proximal helix with two gyres was present beneath the transitional plate (Honda *et al.*, 1995). Gene sequences from *Sulcochrysis biplastida* have never been determined and thus a phylogenetic inference is still pending for this taxon.

Systematics of Pelagophyceae – why a new order for Plocamiomonas?

Browsing through the characters of selected and yet diverse assemblage of pelagophytes included in Table 2 it became clear that the distribution of character states formed a complex mosaic. For instance, the bi-layered theca, thought to be a defining trait of the Sarcinochrysidales (Wetherbee *et al.*, 2023) can no longer serve as a distinctive feature of this order because it is also observed in *Plocamiomonas*. Consequently, the classification of Sarcinochrysidales relies solely on molecular data. Most species belonging to Pelagomonadales possess a theca with either 4 or 5 layers (*Pelagomonas* being the exception with only a single layer (Wetherbee *et al.*, 2023)) and this, besides molecular data, may further characterize them morphologically.

With specific reference to *Plocamiomonas* it possessed a suite of morphological characters that did not match any of the two existing pelagophyte orders (Table 2) and we therefore proposed a new order. This conclusion was also supported by the phylogenetic inference, where Plocamiomonadales formed a monophyletic evolutionary lineage with high statistical branch support. It is noteworthy to mention that *Plocamiomonas* did not produce a gel matrix, a characteristic feature of Sarcinochrysidales (Han *et al.*, 2018) and that it possessed flagellar roots which appear to be lacking in Pelagomonadales.

Novel feature of Plocamiomonas

The arm-like structures emanating from the cell surface were not supported by microtubules. This arrangement has not been observed in other species of Pelagophyceae and therefore represents a unique feature of *Plocamiomonas*. Arm-like structures protruding from cell surfaces have been observed in the dictyochophytes, the sister group to Pelagophyceae but they should not be considered homologous. In the silicoflagellate *Dictyocha speculum* (Moestrup & Thomsen, 1990) and the pedinellids *Mesodinella arctica* (Daugbjerg, 1996) and *Pteridomonas danica* (Patterson & Fencel, 1985) arms are supported by triads of microtubules. Internally the triads of microtubules terminate close to the nuclear membrane. At least in *P. danica* these arms function as the site for food catchment. Due to the presence of microtubules the arms in dictyochophytes are also called axopodia (Hausmann *et al.*, 2003). The function of the arm-like structures in *Plocamiomonas* is currently undetermined. As food vacuoles containing for example bacteria were never observed during transmission electron microscopy, we are reluctant to suggest that the arm-like structures are involved in phagotrophy.

The 0.5–0.6 µm long thin filament between the proximal part of the central axonemes and the short electron-dense thickening above the transitional plate also represented a unique feature not just in Pelagophyceae but among phytoflagellates in general. Typically, the central axonemes approach close to where the flagellum enters the cell body, also known as the flagellar transition region. Interestingly, a central thickening was also noted for *Ankylochrysis* (Honda & Inouye, 1995). However, here the thickening consisted of two electron-dense structures and there was only a short gap between these and the central axonemes. The function of the thin filament is not understood.

Autecology

Based on the results of the autecological study *Plocamiomonas psychrophila* represented a euryhaline

marine nanoflagellate. However, it had a higher growth rate at salinities lower than typically seen for surface waters of Baffin Bay during summer (salinity range 30.5–33.1, Mensah *et al.*, 2023). The adaptation to lower salinities fitted well with *P. psychrophila* being isolated from a surface pocket produced by early onset sea ice melt where salinities would be variable. During early summer salinities just below the ice range from 16–22 (Smith *et al.*, 2022) and would represent a likely habitat for pelagic cells. From the temperature experiment we concluded that *P. psychrophila* was a stenothermal cold-water species. It thrived significantly better at 3.8°C compared with 6.8°C (Supplementary fig. S11). At the higher temperature cell abundances never exceeded 5700 ml^{-1} whereas this number reached 80 000 cells ml^{-1} at 6.8°C (Supplementary fig. S12). The experimental periods were identical (10 days). From the pH study it was concluded that future ocean acidification of sea surface waters will most likely not hamper the growth of *P. psychrophila*. At the two respective temperatures tested it grew equally well at all pH levels (7.3, 7.7 and 8.1) (Supplementary fig. S11). Microalgae kept in culture for long periods of time (several years/decades) have been shown to select for tolerance to high pH and low growth rates (e.g. Berge *et al.*, 2012). Yet large intraspecific variation has been noted. The strain examined here had been cultured for 18 years before the autecological studies were performed. During this time selection for tolerance to high pH values was expected due to the recurrent events of high pH between dilutions with fresh medium. However, here we explored the tolerance to lower pH values and observed similar growth over the range provided. The nearly two decades of maintaining the culture in growth media with a salinity of 30 also did not seem to have selected against growth at lower salinities as the strain grew better at lower salinities ranging from 5–25 compared with 30. See Supplementary document S1 for an extended discussion of the autecological study.

Future studies

Future studies of *P. psychrophila* should focus on ultrastructure of the cell covering using high-pressure freezing and thus examine if micro- or macropores (or both types) are present in layer 2 of the theca. Additionally, it would be interesting to reveal if thecal material is deployed in a similar manner to one of the two ways known in the Pelagophyceae (Wetherbee *et al.*, 2023) or if a third mechanism is used. In the context of *Plocamiomonas psychrophila* and the eight closely related uncultured clones additional studies should address their ecological status as cold-water species. This would require isolating some of these for subsequent in-depth studies of their environmental acclimation and behaviours.

Acknowledgements

We thank Lis Munk Frederiksen for thin sectioning of the material and Øjvind Moestrup for discussions on flagellar features in nanoflagellates. We also thank Marianne Potvin for culture maintenance at Laval University and cell preparation for confocal microscopy. John F. Steffensen is thanked for sharing his experience with precise adjustments of water temperatures using a relay-based system. Two anonymous reviewers provided helpful comments to an earlier version of the manuscript.

Disclosure statement

No potential conflict of interest was reported by the author(s).

Funding

ND thanks Carlsbergfondet [grant numbers 2012_01_0509 and 2013_01_0259] and Brødrene Hartmann Fonden [grant number A22920] for equipment grants. This study was also supported by the Natural and Science Engineering Council (NSERC) Canada, Discovery Grant to CL.

Supplementary material

The following supplementary material is accessible via the Supplementary Content tab on the article's online page at https://doi.org/10.1080/09670262.2024.2353940.
Supplementary table S1. AICB_strains
Supplementary table S2. Coenobium type and the morphological parameters
Supplementary table S3. Comparisons of the coenobium type
Supplementary table S4. The Paired Samples T-Test
Supplementary table S5. ANOVA
Supplementary table S6. The Post Hoc coenobium types of the two strains
Supplementary table S7. The matrix of ranked dissimilarities
Supplementary table S8. Statistical analysis of morphological parameters
Supplementary figure S1. ML_2D_phylogenetic_tree
Supplementary figure S2. ASAP_tree
Supplementary figure S3. PTP_tree
Supplementary figure S4. GMYC_tree
Supplementary figure S5. ITS2 secondary structureFigure S6_SSU 18S_phylogenetic_tree
Supplementary dataset S1. CBC_matrix

Author contributions

N. Daugbjerg: original concept, microscopy, phylogeny, autecology, funding, drafting and editing manuscript; C. Lara: autecology and editing manuscript; F.F. Gai: autecology and editing manuscript; C. Lovejoy: sampling, pigments, chloroplast 3D, sequencing, funding, editing manuscript.

ORCID

Niels Daugbjerg http://orcid.org/0000-0002-0397-3073
Cecilie Lara http://orcid.org/0000-0003-4645-1336
Frederik F. Gai http://orcid.org/0009-0002-1955-820X
Connie Lovejoy http://orcid.org/0000-0001-8027-2281

References

Ali, A.B., De Baere, R., De Wachter, R. & Van de Peer, Y. (2002). Evolutionary relationships among heterokont algae (the autotrophic stramenopiles) based on combined analyses of small and large subunit ribosomal RNA. *Protist*, **153**: 123–132.

Andersen, R.A., Saunders, G.W., Paskind, M.P. & Sexton, J. P. (1993). Ultrastructure and 18S rRNA gene sequence for *Pelagomonas calceolate* gen. et sp. nov. and the description of a new algal class the Pelagophyceae classis nov. *Journal of Phycology*, **29**: 701–715.

Berge, T., Daugbjerg, N. & Hansen, P.J. (2012). Isolation and cultivation of microalgae select for low growth rate and tolerance for high pH. *Harmful Algae*, **20**: 101–110.

Cavalier-Smith, T. & Chao, E.E.-Y. (2006). Phylogeny and megasystematics of phagotrophic heterokonts (kingdom Chromista). *Journal of Molecular Evolution*, **62**: 388–420.

Daugbjerg, N. (1996). *Mesopedinella arctica* gen. et sp. nov. (Pedinellales, Dictyochophyceae) I: fine structure of a new marine phytoflagellate from Arctic Canada. *Phycologia*, **35**: 435–445.

Daugbjerg, N. & Andersen, R.A. (1997). A molecular phylogeny of the heterokont algae based on analyses of chloroplast-encoded *rbc*L sequence data. *Journal of Phycology*, **33**: 1031–1041.

Daugbjerg, N., Jensen, M.H. & Hansen, P.J. (2013). Using nuclear-encoded SSU and LSU rRNA gene sequences to identify the eukaryotic endosymbiont in *Amphisolenia bidentata* (Dinophycea). *Protist*, **164**: 411–422.

Daugbjerg, N. & Moestrup, Ø. (1992*a*). Ultrastructure of *Pyramimonas cyrtoptera* sp. nov. (Prasinophyceae), a species with 16 flagella from northern Foxe Basin, Arctic Canada, including observations on growth rates. *Canadian Journal of Botany*, **70**: 1259–1273.

Derelle, R., Lopez-Garcia, P., Timpano, H. & Moreira, D. (2016). A phylogenetic framework to study the diversity and evolution of stramenopiles (= Heterokonts). *Molecular Biology and Evolution*, **33**: 2890–2898.

DeYoe, H.R., Stockwell, D.A., Bidigare, R.R., Latasa, M., Johnson, P.W., Hargraves, P.E. & Suttle, C.A. (1997). Description and characterization of the algal species *Aureoumbra lagunensis* gen. et sp. nov. and referral of *Aureoumbra* and *Aureococcus* to the Pelagophyceae. *Journal of Phycology*, **33**: 1042–1048.

Freyria, N.J., Kuo, A., Chovatia, M., Johnson, J., Lipzen, A., Barry, K.W., Grigoriev, I.V. & Lovejoy, C. (2022). Salinity tolerance mechanisms of an Arctic pelagophyte using comparative transcriptomic and gene expression analysis. *Communications Biology*, **5**: 500.

Gayral, P. (1972). Sur les Chrysophycées à zoïdes phéophycéens, notamment *Sarcinochrysis marina* Geitler. *Bulletin Société Phycologique De France*, **17**: 40–45.

Gayral, P. & Billard, C. (1986). A survey of the marine chrysophyceae with special reference to the sarcinochrysidales. In *Chrysophytes: aspects and problems* (Kristensen, J. & Andersen, R.A., eds.), 37–48. Cambridge University Press, Cambridge, UK.

Guillard, R.R.L. & Hargraves, P.E. (1993). *Stichochrysis immobilis* is a diatom, not a chrysophyte. *Phycologia*, **32**: 234–236.

Guindon, S., Dufayard, J.F., Lefort, V., Anisimova, M., Hordijk, W. & Gascuel, O. (2010). New algorithms and methods to estimate maximum-likelihood phylogenies: assessing the performance of PhyML 3.0. *Systematic Biology*, **59**: 307–321.

Hamilton, A.K., Lovejoy, C., Galand, P.E. & Ingram, R.G. (2008). Water masses and biogeography of picoeukaryote assemblages in a cold hydrographically complex system. *Limnology and Oceanography*, **53**: 922–935.

Han, K.Y., Graf, L., Reyes, C.P., Melkonian, B., Andersen, R.A., Yoon, H.S. & Melkonian, M. (2018). A re-investigation of *Sarcinochrysis marina* (Sarcinochrysidales, Pelagophyceae) from its type locality and the descriptions of *Arachnochrysis, Pelagospilus, Sargassococcus* and *Sungminbooa* genera nov. *Protist*, **169**: 79–106.

Hausmann, K., Hülsmann, N. & Radek, R. (2003). *Protistology*. 3rd ed. E. Schweizerbart'sche Verlagsbuchhandlung, Berlin, Stuttgart.

Honda, D. & Inouye, I. (1995). Ultrastructure and reconstruction of the flagellar apparatus architecture in *Ankylochrysis lutea* (Chrysophyceae, Sarcinochrysidales). *Phycologia*, **34**: 215–227.

Honda, D., Kawaichi, M. & Inouye, I. (1995). *Sulcochrysis biplastida* gen. et sp. nov.: cell structure and absolute configuration of the flagellar apparatus of an enigmatic chromophyte alga. *Phycological Research*, **43**: 1–16.

Lewin, J., Norris, R.E., Jeffrey, S.W. & Pearson, B.E. (1977). An aberrant chrysophycean alga *Pelagococcus subviridis* gen. nov. et sp. nov. from the North Pacific Ocean. *Journal of Phycology*, **13**: 259–266.

Lobban, C.S., Honda, D., Chihara, M. & Schefter, M. (1995). *Chrysocystis fragilis* gen. nov. sp. nov. (Chrysophyceae, Sarcinochrysidales), with notes on other macroscopic chrysophytes (golden algae) on Guam reefs. *Micronesica*, **28**: 91–102.

Majaneva, M., Rintala, J.M., Piisila, M., Fewer, D.P. & Blomster, J. (2012). Comparison of wintertime eukaryotic community from sea ice and open water in the Baltic Sea, based on sequencing of the 18S rRNA gene. *Polar Biology*, **35**: 875–889.

Mensah, V., Fujita, K., Howell, S., Ikeda, M., Komatsu, M. & Ohshima, K.I. (2023). Estimation of ice melt, freshwater budget, and their multi-decadal trends in the Baffin Bay and Labrador Sea. *Egusphere*, 2023-2492. (preprint). https://egusphere.copernicus.org/preprints/2023/egusphere-2023-2492/

Moestrup, Ø. & Thomsen, H.A. (1980). Preparation of shadow-cast whole mounts. In *Handbook of phycological methods: developmental & cytological methods* (Gantt, E., editor), 385–390. Cambridge University Press, Cambridge, UK.

Moestrup, Ø. & Thomsen, H.A. (1990). *Dictyocha speculum* (Silicoflagellata, Dictyochophyceae), studies on armoured and unarmoured stages. *The Royal Danish Academy of Sciences and Letters, Biologiske Skrifter*, **37**: 1–56.

Patterson, D.J. & Fencel, T. (1985). Insights into the evolution of heliozoa (Protozoa, Sarcodina) as provided by ultrastructural studies on a new species of flagellate from the genus *Pteridomonas*. *Biological Journal of the Linnean Society*, **24**: 381–403.

Riisberg, I., Orr, R.J., Kluge, R., Shalchian-Tabrizi, K., Bowers, H.A., Patil, V., Edvardsen, B. & Jakobsen, K.S. (2009). Seven gene phylogeny of heterokonts. *Protist*, **160**: 191–204.

Ronquist, F. & Huelsenbeck, J.P. (2003). MrBayes 3: bayesian phylogenetic inference under mixed models. *Bioinformatics*, **19**: 1572–1574.

Roy, S., Llewellyn, C.A., Egeland, E.S. & Johnsen, G. (2011). *Phytoplankton pigments: characterization, chemotaxonomy and applications in oceanography*. Cambridge University Press, Cambridge, United Kingdom.

Sieburth, J.M., Johnson, P.W. & Hargraves, P.E. (1988). Ultrastructure and ecology of *Aureococcus anophagefferens* gen. et sp. nov. (Chrysophyceae): the dominant picoplankter during a bloom in Narragansett Bay, Rhode Island, summer 1985. *Journal of Phycology*, **24**: 416–425.

Smith, M.M., von Albedyll, L., Raphael, I.A., Lange, B.A., Matero, I., Salganik, E., Webster, M.A., Granskog, M.A., Fong, A., Lei, R. & Light, B. (2022). Quantifying false bottoms and under-ice meltwater layers beneath Arctic summer sea ice with fine-scale observations. *Elementa Science of the Antropocene*, **10**: 000116.

Swofford, D.L. (2002). *PAUP*: phylogenetic analysis using parsimony (* and other methods), version 4*. Sinauer Associates, Sunderland, Massachusetts.

Thakur, R., Shiratori, T. & Ishida, K.-I. (2019). Taxon-rich multigene phylogenetic analyses resolve the phylogenetic relationship among deep-branching stramenopiles. *Protist*, **170**: 125682.

Tian, F., Yu, Y., Chen, B., Li, H.R., Yao, Y.F. & Guo, X.K. (2009). Bacterial, archaeal and eukaryotic diversity in Arctic sediment as revealed by 16S rRNA and 18S rRNA gene clone libraries analysis. *Polar Biology*, **32**: 93–103.

Wetherbee, R., Bringloe, T.T., Costa, J.F., van de Meene, A., Andersen, R.A. & Verbruggen, H. (2021). New pelagophytes show a novel mode of algal colony development and reveal a perforated theca that may define the class. *Journal of Phycology*, **37**: 396–411.

Wetherbee, R., Bringloe, T.T., van de Meene, A., Andersen, R.A. & Verbruggen, H. (2023). Structure and formation of the perforated theca defining the Pelagophyceae (Heterokonta), and three new genera that substantiate the diverse nature of the class. *Journal of Phycology*, **59**: 126–151.

Wetherbee, R., Gornik, S.G., Grant, B. & Waller, R.F. (2015). *Andersenia*, a genus of filamentous, sand-dwelling Pelagophyceae from southeastern Australia. *Phycologia*, **54**: 35–48.

Wetherbee, R., Jackson, C.J., Repetti, S.I., Clementson, L.A., Costa, J.F., van de Meene, A., Crawford, S. & Verbruggen, H. (2019). The golden paradox – a new heterokont lineage with chloroplasts surrounded by two membranes. *Journal of Phycology*, **55**: 257–278.

Wu, W., Wang, L., Liao, Y. & Huang, B. (2015). Microbial eukaryotic diversity and distribution in a river plume and cyclonic eddy-influenced ecosystem in the South China Sea. *Microbiology Open*, **4**: 826–840.

Yang, E.C., Boo, G.H., Kim, H.J., Cho, S.M., Boo, S.M., Andersen, R.A. & Yoon, H.S. (2012). Supermatrix data highlight the phylogenetic relationships of photosynthetic stramenopiles. *Protist*, **163**: 217–231.

Zapata, M., Rodrígue, Z.F. & Garrido, J.L. (2000). Separation of chlorophylls and carotenoids from marine phytoplankton: a new HPLC method using a reversed phase C8 column and pyridine-containing mobile phase. *Marine Ecology Progress Series*, **195**: 29–45.

Zhu, J., Hu, J. & Zheng, Q. (2022). An overview on water masses in the China seas. *Frontiers in Marine Science*, **9**: 972921.